ARTICLE

Plasma-Based Surface Modification of Polystyrene Microtiter Plates for Covalent Immobilization of Biomolecules

Stella H. North,[†,‡] Evgeniya H. Lock,[*,†,§] Candace J. Cooper,[§] James B. Franek,[§,⊥] Chris R. Taitt,[‡] and Scott G. Walton[§]

Center for Bio/Molecular Science & Engineering and Plasma Physics Division, U.S. Naval Research Laboratory, 4555 Overlook Avenue SW, Washington, D.C. 20375, United States, and Global Strategies Group (North America), Inc., Crofton, Maryland 21114, United States

ABSTRACT In recent years, polymer surfaces have become increasingly popular for biomolecule attachment because of their relatively low cost and desirable bulk physicochemical characteristics. However, the chemical inertness of some polymer surfaces poses an obstacle to more expansive implementation of polymer materials in bioanalytical applications. We describe use of argon plasma to generate reactive hydroxyl moieties at the surface of polystyrene microtiter plates. The plates are then selectively functionalized with silanes and cross-linkers suitable for the covalent immobilization of biomolecules. This plasma-based method for microtiter plate functionalization was evaluated after each step by X-ray photoelectron spectroscopy, water contact angle analysis, atomic force microscopy, and bioimmobilization efficacy. We further demonstrate that the plasma treatment followed by silane derivatization supports direct, covalent immobilization of biomolecules on microtiter plates and thus overcomes challenging issues typically associated with simple physisorption. Importantly, biomolecules covalently immobilized onto microtiter plates using this plasma-based method retained functionality and demonstrated attachment efficiency comparable to commercial preactivated microtiter plates.

KEYWORDS: polystyrene • microtiter plate • argon plasma • silanization • surface characterization • surface functionalization

INTRODUCTION

Manufacture of microtiter plates used in clinical diagnostics, environmental monitoring, biotech, pharmaceutical research and development, and many other areas of basic and applied research represents a half-billion dollar enterprise. Microtiter plates are effective solid-phase platforms for multiplexed, high-throughput screening and analysis of biomolecule interactions. This multiwell format, available in 6, 24, 96, 384, 1536, and even 3456 or 9600-well plates, is widely used in both industry and medical fields because of its ease of automation, high capacity for paralleled data collection, and versatile application of technologies (e.g., proteomics, functional genomics, biomolecule separation, and purification).

Microtiter plates are manufactured using a variety of polymeric materials (e.g., polypropylene, polycarbonate), but polystyrene (PS) is most commonly employed because it readily adsorbs (via noncovalent interaction) proteins, has excellent optical as well as mechanical properties, and is cost-effective. However, several intrinsic properties of polystyrene also present disadvantages: poor chemical resistance, difficulty controlling surface chemistry, but most importantly, the simple physisorption can lead to protein denaturation, desorption and/or loss of biomolecule activity (1, 2). The benefits of the covalent attachment versus physisorption of biomolecules are largely recognized. It represents a more robust approach that can ensure a more stable attachment and functional display of the biomolecule of interest (3).

Covalent attachment of biomolecules to polymer surfaces can be achieved using a variety of techniques including wet chemical treatments, silane monolayers, plasmas, flames, and UV irradiation (3). The use of wet chemical treatments alone or as a pretreatment step to render the polystyrene substrates amenable to silane functionalization can lead to the production of a wide range of oxygen-containing functional groups (e.g., C═O, O−C═O, CO_3), and thus nonspecific biomolecule attachment (4). Polymers treated in this manner may, therefore, be less useful for applications that require more specific functionalities. Moreover, harsh surface treatments can lead to irregular surface etching, which can play a significant role in modulating the efficacy of bioimmobilization and functionality of the biointerface.

The use of plasmas as means of polymer thin film deposition, polymer surface treatment by a variety of gases (Ar, O_2, N_2, NH_3, $N_2 + H_2$, CO_2, etc.) to introduce desired functional groups and plasma grafting methods have been a preferred way for covalent biomolecules immobilization as signified by the numerous publications in this field (5−9). However, chemical modifications produced by plasmas and UV treatments are often accompanied by surface morphol-

* Corresponding author. Phone: (202) 767-0351. Fax: (202) 763-7531. E-mail: evgeniya.lock@nrl.navy.mil.

Received for review June 29, 2010 and accepted September 13, 2010

† These authors contributed equally to this work.

‡ Center for Bio/Molecular Science & Engineering, U.S. Naval Research Laboratory.

§ Plasma Physics Division, U.S. Naval Research Laboratory.

⊥ Global Strategies Group (North America).

DOI: 10.1021/am100566e

Published on Web 09/29/2010

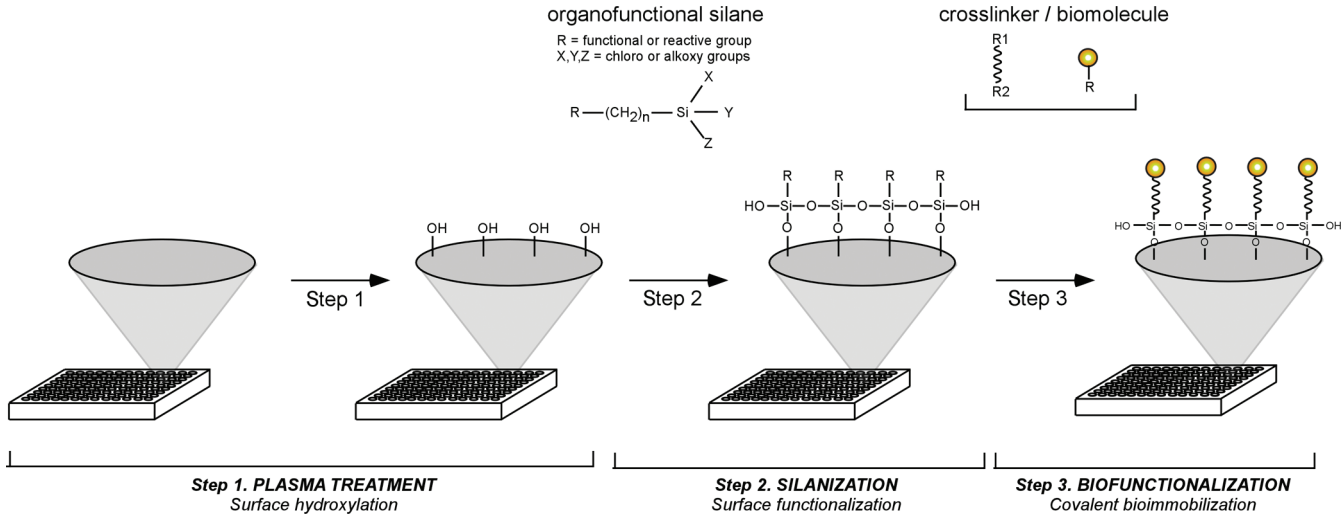

FIGURE 1. Schematic illustration of plasma-induced surface functionalization of polystyrene microtiter plate. The method is comprised of three steps: step 1, argon plasma-induced surface modification with reactive hydroxyl groups; step 2, silanization using organofunctional silane; step 3, bioimmobilization either directly with indirectly with the use of intermediate cross-linkers.

ogy modifications. Surface morphology has been shown to affect the activity of the immobilized biomolecules and surface energy of core substrates (10−12), and significantly alter the biophysical and biochemical behavior of the bio-interface (13, 14). The ultimate goal of this work is to immobilize small biomolecules such as peptides, saccharides, and small proteins, which are highly sensitive to their microenvironment (15−18). Thus precise control over not only the surface chemistry but also the surface morphology at the nanoscale is required. The electron beam plasma has shown the ability to functionalize polymer surfaces while keeping the surface morphology unchanged (19).

In this work, to further increase the selectivity of biomolecules attachment and to provide better structural order, we used silane coupling chemistry in addition to plasma treatment of the polystyrene microtiter plates. Two other groups, Kaur et al. (4) and Darain et al. (20) have described procedures for bioimmobilization on silanized polystyrene supports for use in enzyme-linked immunosorbent assays. The first study uses chemical pretreatment prior to silanization and provides limited characterization of the polymer surface. Darain et al. (20) suggest using UV/ozone treatment in conjunction with silanes to covalently immobilize biomolecules. However, their work shows significant change in polymer surface morphology after UV irradiation, and thus it might not be applicable to immobilization of small biomolecules.

In this paper, we describe a method for the surface modification of polystyrene microtiter plates that consists of three distinct but dependent steps, comprising both dry and wet chemical processing, to yield a versatile, covalent immobilization platform for biomedical and biological applications (Figure 1) (1): plasma-based introduction of surface hydroxyl groups (2), silane monolayer assembly using organo-functional silanes, and finally (3), covalent coupling of the biomolecule of interest using cross-linkers of variable functionality and spacer length for user-defined surface characteristics. The surfaces are analyzed after each step by water contact angle measurements, X-ray photoelectron spectroscopy, and atomic force microscopy. The efficacy of biomolecule immobilization was also extensively characterized. In addition, peptide immobilization onto treated polymers and glass slides was compared and the results suggest the ability to use the same biomolecular immobilization procedures for both substrates.

EXPERIMENTAL SECTION

Materials. Microfluor I and NUNC Immobilizer Amino 96-well microtiter plates were obtained from Thermo Fisher Scientific (Rochester, NY). Rabbit anti-lipid A (*Escherichia coli*) IgG was purchased from AbD Serotec (Raleigh, NC). Antimicrobial peptides (AMPs) cecropin A, cecropin P1, melittin, and cecropin A(1−8)-melittin (1−18) amide were received from American Peptide Company, Inc. (Sunnyvale, CA). Cy3 monofunctional *N*-hydroxysuccinimidyl ester, 4-maleimidobutyric acid *N*-hydroxysuccinimide ester (GMBS), and bis(sulfosuccinimidyl) suberate (BS^3) were purchased from Amersham-Pharmacia (Piscataway, NJ). Lipopolysaccharide (LPS) from *Salmonella typhimurium*, (3-mercaptopropyl)triethoxysilane (MTPES), (3-aminopropyl)triethoxysilane (APTES), phosphate buffered saline (PBS), pH 7.4, potassium hydroxide, Tween-20, bovine serum albumin (BSA), dimethyl sulfoxide (DMSO), and methanol were purchased from Sigma-Aldrich (St. Louis, MO).

Preparation of Fluorescently Labeled IgG and LPS. Rabbit IgG and LPS were conjugated with Cy3 monoreactive dye following manufacturer's instructions. Briefly, one mg IgG or LPS in 50 mM sodium borate, pH 8.5 was incubated with one packet of Cy3 monoreactive dye, previously dissolved in 25 μL anhydrous DMSO. After 1 h incubation at room temperature, the labeled IgG and LPS were purified from unincorporated dye by gel filtration on BioGel P-10 and BioGel P-2, respectively (BioRad, Hercules, CA). The labeled biomolecules were stored in the dark at 4 °C until use. The molar ratios of dye to labeled species ranged from 1.7 to 3.5 for antibodies and 1.1 to 1.4 for LPS.

Water Contact Angle (WCA) Measurements. Goniometry was performed using a static sessile drop technique on microtiter plate fragments. Contact angle measurements were performed at room temperature using a goniometer (AST Products, Inc.), equipped with a microsyringe to control volume of the liquid drop (2 μL). Four water drops were placed at different locations on each substrate surface. Eight contact angle mea-

surements (each side of one water drop) were averaged and corresponding standard deviation were calculated for each plate fragment.

X-ray Photoelectron Spectroscopy (XPS). Surface elemental and chemical state analyses were performed on a K-Alpha X-ray photoelectron spectrometer (Thermo Scientific). This instrument is equipped with a microfocusing monochromator (Al−Kα X-ray source, 1486.6 eV), which was operated at a spot size of 400 μm. Analyzer pass energies of 200 and 25 eV respectively were used for elemental survey and chemically sensitive narrow scan spectra. The detection angle was 0°, which provides average analyzed depth down to 10 nm. K-Alpha's charge compensation system was used during the analysis, utilizing very low energy electrons and argon ions to prevent any localized charge build-up. Spectra were referenced to the main C 1s peak at 285.0 eV and quantified using Scofield sensitivity factors. The high-resolution elemental spectra were fitted using a commercial XPS analysis software package Unifit as previously described (21). Briefly, the multiple-component fitting in the C 1s region always started from the lowest binding energy component and its full width at half-maximum was allowed to vary. A convolution of Gaussian and Lorentzian line shapes was assumed for individual peaks, following the line shape parametrization. To produce consistent fits of minor C 1s components, their widths were constrained to the FMHW of the first peak and their positions were assigned as follows C−CO_2 285.7 eV, C−O 286.6 eV, C═O 287.6 eV, and O−C═O 289 eV. A linear combination of Shirley and linear functions with consistent parameters was used to model the background.

Atomic Force Microscopy (AFM). The polymer surface morphology was examined using an atomic force microscope (Nanoscope III, Veeco Metrology, Santa Barbara, CA) operated in tapping mode. Surface images were obtained from $5 \times 5\,\mu m^2$ scans at resolution of 256 × 256 pixels and scan rate of 1 Hz. For a quantitative evaluation of the topography changes, root-mean-square (rms) roughness was calculated from the surface height data z_i using

$$R_q = \left[\frac{1}{N}\sum_{i=1}^{N}|z_i - \bar{z}|^2\right]^{1/2}$$

where $\bar{z}$ is the mean height.

Plasma Treatment of Microtiter Plates. The experimental apparatus has been discussed previously (22). The system vacuum was maintained by a 250 L/s turbo pump, with a base pressure of 5×10^{-6} Torr. The operating pressure was achieved by introducing argon (purity >99.9999%), through mass flow controllers and by throttling the pumping speed using a manual gate valve. The electron beam was produced by applying a −2 kV pulse to a linear hollow cathode for a selected pulse width and duty factor. The emergent beam passed through a slot in a grounded anode and was then terminated at a second grounded anode located further downstream. Beam spreading from collisions with the background gas was suppressed by a coaxial magnetic field (150 G) produced by a set of external coils. The microtiter plates were placed on a 10.2 cm diameter stage located at 2.5 cm from the nominal edge of the electron beam. The stage was held at ground potential and room temperature.

All of the treatments were conducted at a pressure of 90 mTorr. The total gas flow rate was held constant at 50 sccm. The exposure time was 2 min. The plasma period was 20 ms and the duty factor was 10%. The period is defined as the time between two consecutive pulses, comprising the beam pulse width (when plasma is produced), the afterglow (when plasma decays), and the time when no plasma is present; the duty factor is defined as the ratio of the plasma on-time to the period.

Microtiter Plate Silanization and Immobilization of IgG. NUNC Microfluor I 96-well microtiter plates were rinsed with methanol prior to silanization. Microwells were covered with 100 μL of 2% silane solution (MPTES or APTES) prepared in methanol adjusted to pH 4 by addition of several drops acetic acid. After 30 min of incubation under nitrogen, plates were removed, rinsed three times in methanol, and dried. Cross-linking was performed by covering microwells with 100 μL of 1.0 mM GMBS in absolute ethanol and incubating for 30 min. Alternatively, 100 μL of 50 mM BS^3 in 10 mM phosphate buffer, pH 6.0, was used. Plates were rinsed thrice with 200 μL deionized water and dried; 1 μg/mL, 3 μg/mL, or 10 μg/mL Cy3-labeled antibody (in PBS) was then added into each microwell and allowed to incubate for 2 h at room temperature with gentle agitation; each concentration was patterned in quadruplicate. Each microwell was washed three times with 250 μL of PBS with 0.005% Tween 20 (PBST). One-hundred microliters of PBS was added to each microwell and the plate was read on a Tecan Safire microplate reader.

Immobilization of Peptides and LPS Binding Assay. Microwells were covered with 100 μL of 2% mercaptosilane solution prepared in acidic methanol and incubated for 30 min under nitrogen. Cross-linking was accomplished by covering microwells with 100 μL of 1.0 mM GMBS in absolute ethanol and incubated for an additional 30 min. One-hundred microliters of antimicrobial peptide solution (250 μg/mL in PBS) was added to each well and allowed to incubate at room temperature for 2 h with gentle agitation; each peptide was patterned in quadruplicate. For detection, after three washes with PBST, each well received 100 μL of Cy3-conjugated LPS and was incubated for 2 h at room temperature with gentle agitation. After this time, each microwell was washed three times with PBST; 100 μL PBS was added to each microwell and the plate was read on the Tecan microplate reader. For comparison of binding patterns, peptides were also immobilized onto standard glass slides as previously described using MPTES and GMBS (23, 24). Cy3-labeled LPS was applied to the glass-immobilized peptides and incubated for 2 h, prior to washing with PTST and imaging using a Packard ScanArray Lite confocal microarray scanner; data were extracted from images using QuantArray microarray analysis software. To emphasize the differences in the patterns of binding, as well as to account for disparity in measurements obtained on the two instruments (microarray scanner, microtiter plate reader), data from both microtiter plates and glass slides were normalized with respect to LPS-melittin binding.

RESULTS AND DISCUSSION

Microtiter plates were exposed to pulsed, electron beam generated plasma produced in argon to activate the plate surface by generating oxygen-based functional groups (Figure 1, step one). OH-Enriched, plasma-modified surfaces were then treated with (3-mercaptopropyl)triethoxysilane (MPTES) or 3-aminopropyltriethoxysilane (APTES) to yield a surfaces functionalized with pendant thiol or amine moieties, respectively (step two), for subsequent immobilization of biomolecules via commercial bifunctional cross-linkers (step three). Surfaces were characterized before and after plasma treatment, and after silanization, using X-ray photoelectron microscopy (XPS) and water contact angle (WCA) measurements. Efficiency of bioimmobilization was measured after cross-linking by measuring fluorescence of attached fluorophore-labeled antibodies, or alternatively, through binding studies of immobilized antimicrobial peptides, previously demonstrated to capture bacterial cells and cellular markers when immobilized on silane-treated surfaces (15, 23).

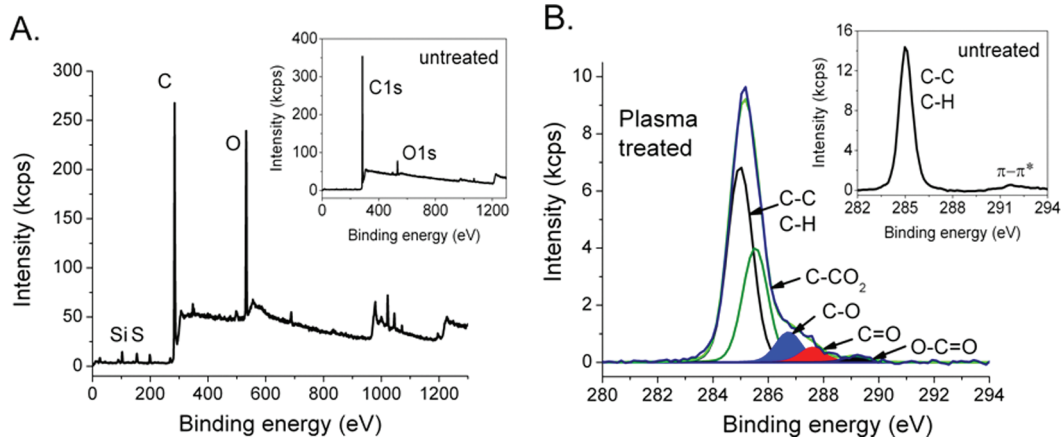

FIGURE 2. (A) XPS survey spectra and (B) high-resolution C1s region of plasma-treated and untreated (inset) microtiter plate fragments.

Table 1. Ralative Atomic Concentrations (%) and Standard Deviations[a] of the Measured Elements, Water Contact Angles (WCA), and Roughness (RMS) Values of Mercaptotosilanized Polystyrene Microtitre Plate before and after Argon Plasma Treatment

substrate	MPTES	C	O	Si (102.3 eV)	S (163 eV)	WCA (deg)[b]	rms
MT plate	−	92.8 ± 1.4	5.3 ± 1.0	1.2 ± 0.6	0.3 ± 0.3	95.9 ± 4.6	7.0 ± 1.7
MT plate	+	82.7 ± 0.6	12.3 ± 1.0	0.5 ± 0.1	1.3 ± 0.1	81.9 ± 10.1	8.3 ± 2.4
MT plate, plasma treated	-	80.9 ± 0.4	16.3 ± 0.3	0.4 ± 0.1	ND[c]	48.7 ± 4.4	7.1 ± 1.7
MT plate, plasma-treated	+	72.2 ± 1.1	16.5 ± 1.3	4.3 ± 0.3	4.0 ± 0.3	60.1 ± 2.1	7.9 ± 0.5

[a] Values represent means of three determinations ± standard deviation. [b] Value represents mean ± standard error of four averages at different locations. [c] ND, not dectected.

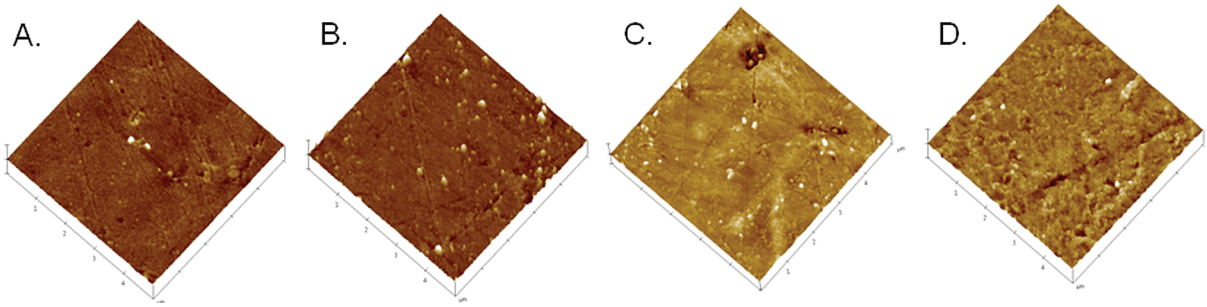

FIGURE 3. AFM images of (A) untreated, (B) untreated silanized, (C) plasma-treated, and (D) plasma-treated silanized microtiter plates.

Characterization of Polystyrene Microtiter Plates after Plasma Treatment. As expected, the untreated polystyrene was hydrophobic (WCA of 95.93 ± 4.57°) and showed carbon as the predominant constituent (C1s 92.78 ± 1.43 at. %) (Figure 2A, inset; Table 1). After plasma treatment, the polystyrene surface exhibited a significant increase in oxygen concentration (from 5.3 to 16.26 at. %; $P < 0.005$), with trace levels of silicon (<0.5 at. %) detected as well. The high-resolution C1s spectra (Figure 2B) detailed the plasma-mediated formation of oxygen-based functional groups, including C−O (hydroxyls, ethers) and C═O (epoxy, aldehydes, ketones); the presence of these moieties resulted in an increase in surface hydrophilicity, as confirmed by the 2-fold reduction of the WCA to 48.68 ± 4.37°. The majority of oxygen incorporated into the polymer surface was in the form of singly bonded oxygen; however, C−O was indistinguishable from C−OH in the high-resolution spectra. Gas-phase chemical derivatization analysis (25) based on fluorine labeling using trifluoroacetic anhydride indicated that nearly all of the C−O/C−OH bonds designated in the high resolution C1s spectra were attributed to C−OH bonds (see the Supporting Information). In contrast to reactive gases, plasmas created in inert gas do not directly introduce functional groups to the surface. However, they do promote surface chemistries via the breaking of bonds, generating reactive sites (dangling bonds) where functional groups can attach (19); the incorporation of oxygen occurs at those locations upon sample exposure to air after plasma treatment. In this case, hydroxyl groups were most likely formed because of the dissociative adsorption of water upon exposure to ambient air (26, 27). As previously noted, the incident ion energy is small in electron beam generated plasmas and thus the creation of reactive sites is not accompanied by significant changes in morphology as shown in Figure 3A, 3C ($P > 0.5$, data not shown). Thus, incorporation of functional groups, and not surface roughness, is responsible for the observed changes in water contact angle. As will be discussed later, this unique plasma surface treatment promotes uniform silane layer formation and small peptide immobilization.

Characterization of Polystyrene Microtiter Plates after Silanization. XPS, WCA, and AFM measurements were also used to evaluate the efficiency and uniformity of silanization on plasma-treated and untreated polystyrene surfaces. Because a mercaptosilane was used in the silanization step, the presence of sulfur (−SH, binding energy (BE) at 163 eV) and silicon (O−Si−C, BE at 102.6 eV) in the XPS survey spectra served as indicators for silanization. The sulfur and silicon unique to the silane were differentiated from trace element contaminants in the commercial microtiter plates; sulfur content/contamination from the plates was identified in its oxidized form −SO (BE at 168 eV) and most of the silicon was in the form of Si−O (BE at 103.3 eV) rather than O−Si−C (28).

The XPS results of the silanized, plasma-treated polystyrene surface showed a significant increase in both sulfur and silicon content (≈ 4.0 at. %) compared to the silanized, untreated polystyrene (<1.3 at. %; $P < 0.005$) (Table 1). These results indicated that the silanization efficiency was enhanced by the plasma-induced modification of the polymer surface. WCA of the plasma-treated silanized plate also indicated that silanization occurred; the WCA value changed from 48.68 ± 4.37° (before silanization) to 60.05 ± 2.08° (after silanization) ($P < 0.025$). The increased WCA value is attributed to the hydrophobic alkyl chain in MPTES (29) and is consistent with literature values (20). A moderate (but not significant) change in WCA upon silanization was also observed with plates not treated with plasma ($P > 0.05$). However, the final WCA values observed with untreated, silanized plates showed a larger standard deviation, indicating more heterogeneous surface and presumably less efficient silane deposition. The uniformity of silane deposition was further evaluated by atomic force microscopy. Even though the average roughness values of plasma-treated and untreated silanized polymer plates were approximately the same, the standard deviations in both cases were different; a smaller standard deviation was observed after plasma treatment. Furthermore, a significant globular formation on the surface on the untreated plate is also apparent (cf. Figure 3A with Figure 3B). Silane aggregation was observed by other research groups as well (20). It should be noted that after electron beam plasma treatment, only a few aggregates were observed (Figure 3D).

Biomolecule Immobilization Efficacy. There are many possible permutations of multifunctional and variable length silanes and cross-linkers that can be considered to ensure optimized, tailored attachment of biomolecules to the polystyrene surface. This attachment may take place as a single step, e.g., direct attachment of a biomolecule to a surface functionalized with silane possessing reactive end groups. Alternatively, attachment may be a multistep process, e.g., the indirect attachment of biomolecules through the use of bifunctional cross-linking agents (represented in Figure 1, step three). To demonstrate the suitability of our system for versatile, covalent immobilization of biomolecules to plasma-modified plates, we examined two possible schemes (Figure 4). In scheme one in Figure 4, plasma-

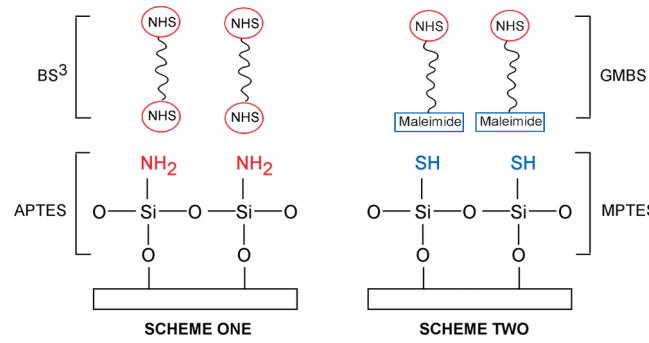

FIGURE 4. Immobilization schemes using aminosilane (left) or mercaptosilane (right).

modified microtiter plates were functionalized with APTES with the intention of presenting surface amine groups. The APTES-treated microwell surfaces were subsequently reacted with an amine-reactive homobifunctional cross-linker (BS^3), which allows the covalent attachment of Cy3-conjugated IgG. In scheme two in Figure 4, MPTES was used to form a silane monolayer presenting surface thiol groups. The MPTES-treated microwell surfaces were then reacted with a heterobifunctional cross-linker (GMBS) followed by the covalent attachment of Cy3-conjugated IgG. In both schemes, untreated polystyrene microtiter plates served as controls. On the basis of the two different immobilization schemes presented, BS^3, which contains two amine-reactive NHS groups, is expected to react only with APTES. GMBS, which displays both an NHS group and a maleimide group that react with amine and sulfhydryl groups, respectively, is expected to react with both APTES and MPTES; however, only the MPTES-GMBS combination is expected promote efficient protein conjugation.

Figure 4 represents the mean net fluorescence values of attached Cy3-IgG (at 1.0, 3.0, and 10 μg/mL) using immobilization Schemes one and two. To fully demonstrate the ability of the plasma-silane cross-linking methodology to enable multiple immobilization strategies on the same plate, we tested APTES-BS^3, MPTES-GBMS, and combinations thereof (i.e., the "wet" chemistry) on the same plasma-treated 96-well plates, or untreated plates as a control. Fluorescent signals on the plasma-treated plate were shown to be significantly higher than the untreated plate (Figure 5, compare panels A and C with panels B and D, respectively; $P < 0.05$). Only low fluorescent signals were detected at even the highest protein concentration tested on the untreated plate; these levels, corresponding to <0.02 pmol/well, are presumably due to background levels of adsorption onto the microtiter plate surface, and are well-below published saturation values for IgG adsorbed to polystyrene (0.35−0.5 pmol/cm^2 (30−32)). Although some immobilization was observed when GMBS was used to cross-link the antibody to APTES-treated plates, Cy3-IgG immobilization on APTES-coated surfaces was much more efficient when BS^3 was used (Figure 5, panel A); GMBS-mediated linking of Cy3-IgG to APTES surfaces may have occurred by reaction with free thiols present on native or partially denatured IgGs, or potentially from low levels of maleimide reaction with excess amines on IgG surfaces (33). On the other hand, bioimmo-

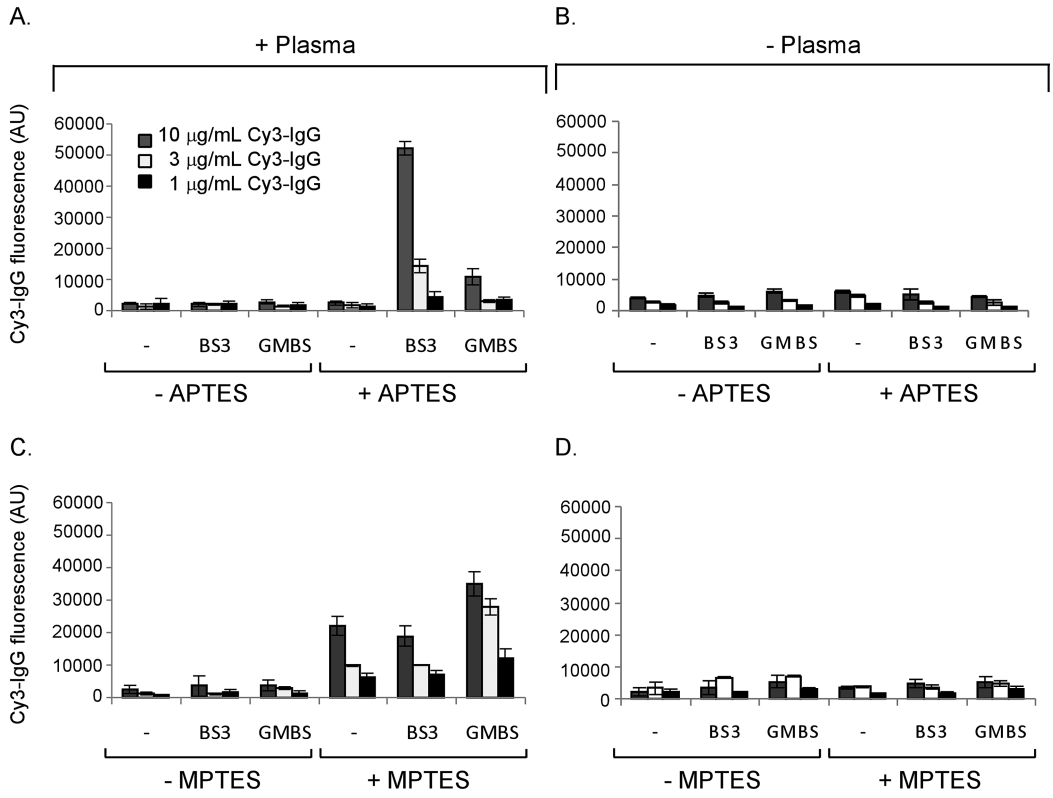

FIGURE 5. Fluorescent intensities of Cy3-IgG binding on plasma-treated (left panels) and untreated (right panels) polystyrene microtiter plates with silanization by APTES (top panels) or MPTES (bottom panels) with BS^3 or GMBS cross-linkers, as indicated.

bilization on MPTES coated surfaces was greatest in the presence of GMBS cross-linker (Figure 5, panel C). Although the MPTES-BS^3 demonstrated higher relative fluorescence, it was comparable to the control samples containing no cross-linker.

IgGs and many other large biomolecules can be immobilized using a wide range of substrates and linking procedures with minimal impact on binding activity. However, smaller biomolecules such as peptides, saccharides, and small proteins are highly sensitive to surface morphology and orientation when immobilized (16–18, 23, 34). To demonstrate that the described chemistry could be applied to this latter category of biomolecules, we utilized a series of naturally occurring antimicrobial peptides as model ligand-binding molecules. These biomolecules are capable of binding to a large variety of microbial cells with different affinities, which makes them useful in detection assays (34); the ability to distinguish between different categories of microbial cells based on their patterns of binding to different peptides can be used for rapid and broad-spectrum screening (15, 23, 24). Previous studies have shown that when immobilized onto glass slides using an amine-directed immobilization strategy (MPTES treatment, followed by GMBS, analogous to scheme two), the peptides displayed unique patterns of binding to Gram-positive and -negative bacteria (35, 36) and to the Gram-negative biomarker lipopolysaccharide, LPS (Figure 6, white bars). Surprisingly, we observed very different patterns of LPS binding when utilizing commercial, preactivated microtiter plates (Immobilizer amino, maleic anhydride; Figure 6, striped bars). Although both types of commercial plates use amine-directed chemistry (as

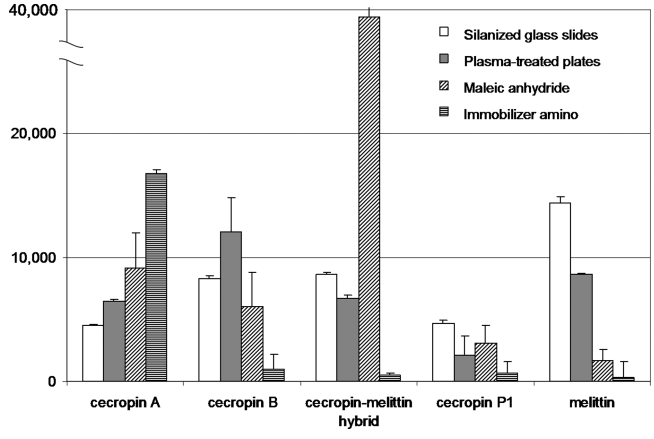

FIGURE 6. Binding of Cy3-LPS by antimicrobial peptides (cecropin A, melittin, cecropin A–melittin hybrid, and cecropin P1) immobilized onto silanized glass slides (white bars), plasma-modified microtiter plates (via MPTES and GMBS, gray bars), and commercial amine-directed, preactivated plates (striped bars). As two instruments were used to obtain and extract fluorescence data (microtiter plate reader, confocal microarray scanner), all values were normalized to those obtained with melittin.

did the glass slides), the differences in reactive groups, overall surface characteristics, and linker lengths appear to affect the immobilized peptides' ability to bind the target LPS, presumably by altering peptide orientation, density, freedom of movement, and/or the number and identity of linked amino acid side chains. However, when plasma-treated plates were processed using analogous chemistry as used on the glass slides (plasma-treatment → silanization with MPTES → cross-linking with GMBS), the binding pattern observed (Figure 6, gray bars) was similar to that of the gold

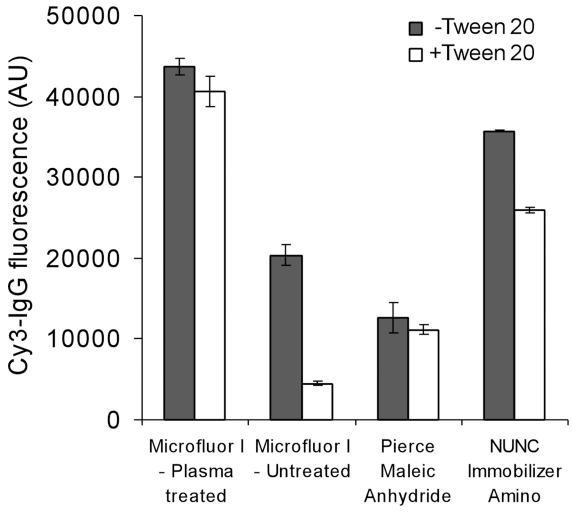

FIGURE 7. Fluorescent intensities of Cy3-IgG (10 μg/mL) immobilization to plasma-treated Microfluor I (covalent immobilization following Scheme Two), Microfluor I (physisorption), Pierce Reactibind Maleic Anhydride, and NUNC Immobilizer Amino (covalent immobilization according to manufacturers' instructions); gray bars = no detergent wash, white bars = detergent wash.

standard glass slides. The ability to transition an immobilization methodology directly from one platform (silanized glass slides) to another (plasma-treated, silanized plates), with minimal alteration of binding specificity, illustrates yet another advantage conferred by the method described here.

Comparison between Plasma-Treated and Commercial Microtiter Plates. The issues of biomolecule denaturation, desorption, and/or loss of biomolecule activity that could occur when biomolecules are immobilized through physisorption have been recognized and not, surprisingly a number of commercial microtiter plate are available in preactivated form for covalent attachment of biomolecules (amine-directed immobilization: Immobilizer Amino and maleic anhydride-functionalized; sulfhydryl-directed immobilization: maleimide-functionalized). We compared the efficacy of biomolecule immobilization (using immobilization scheme two) on plasma-treated, silanized plates, with those of commercial microtiter plates utilizing both physisorption and amine-directed, covalent attachment strategies. Protein immobilization efficiency (fluorescence of immobilized Cy3-IgG) was determined for each kind of plate before and after a stringent detergent wash (buffer with 0.5% Tween-20; Figure 7). Consistent with data presented in Figure 5, plasma-treated plates exhibited significantly higher fluorescent signal than untreated plates (~2-fold increase) where immobilization has occurred via physisorption ("Microfluor I Untreated"; $P < 0.005$). As expected, the difference between the plasma-treated and untreated plates increases dramatically (~8-fold difference) after a detergent wash. Although covalent attachment of IgG to the commercial preactivated plates (Maleic anhydride, NUNC Immobilizer Amino) preserved a greater proportion of the attached biomolecules, the overall binding efficiency of plasma-/silane-treated plates was still superior ($P < 0.01$).

CONCLUSIONS

We have demonstrated that plasma treatment can be combined with silane functionalization to effect the stable and versatile covalent attachment of biomolecules to microtiter plates. The plasma treatment produces uniformly functionalized surfaces with minimal alterations to surface morphology allowing for formation of uniform silane coverage and small peptide immobilization. The silane chemistry provides a facile and controllable covalent immobilization method that can be used to modify and tailor inexpensive polystyrene microtiter plates to display distinctive surface properties or reactive functionalities. Compared to physisorption, covalent attachment avoids desorption and maintains long-term chemical stability of the immobilized biomolecule. Indeed, nearly 95% of the immobilized biomolecules were retained after extensive wash on the plasma-treated surfaces versus 25% of untreated polystyrene microtiter plate. A distinct advantage of the plasma treatment used here is that it allows for small peptide immobilization on polymer substrate. The observed dependences were similar to peptides immobilization on glass slides thus suggesting the capability of using the same silane-based attachment scheme developed for glass slides. Lastly, the plasma-treated plates performed on par or better that commercially available preactivated microtiter plates. However, unlike commercial plates that utilize a single attachment chemistry for all wells, a wide variety of bioimmobilization schemes can be tested on a single plate. Although this work involved polystyrene plates, we suspect that this approach could be used on other polymeric platforms of varying complexities as well.

Acknowledgment. S.H.N. is a recipient of an American Society of Engineering Education postdoctoral fellowship. C.J.C. was supported by an NSF Historically Black Colleges and Universities-Tribal College or University internship program. This work is funded by Joint Science & Technology Office for Chemical & Biological Defense/Defense Threat Reduction Agency and the Office of Naval Research. The views expressed here are those of the authors and do not represent the opinions of the U.S. Navy, the U.S. Department of Defense, or the U.S. government.

Supporting Information Available: Trifluoroacetic anhydride (TFAA) labeling of plasma-treated polystyrene plates explained in detail (PDF). This material is available free of charge via the Internet at http://pubs.acs.org.

REFERENCES AND NOTES

(1) Rebeski, D. E.; Winger, E. M.; Shin, Y.-K.; Lelenta, M.; Robinson, M. M.; Varecka, R.; Crowther, J. R. *J. Immunol. Methods* **1999**, *226*, 85.
(2) Butler, J. E. *Methods* **2000**, *22*, 4.
(3) Goddard, J. M.; Hotchkiss, J. H. *Prog. Polym. Sci.* **2007**, *32*, 698.
(4) Kaur, J.; Singh, K. V.; Raje, M.; Varshney, G. C.; Suri, C. R. *Anal. Chim. Acta* **2004**, *506*, 133.
(5) Desmet, T.; Morent, R.; Geyter, N. D.; Leys, C.; Schacht, E.; Dubruel, P. *Biomacromolecules* **2009**, *10*, 2351.
(6) Chan, C. M.; Ko, T. M.; Hiraoka, H. *Surf. Sci. Rep.* **1996**, *24*, 1.
(7) Bilek, M. M.; McKenzie, D. R. *Biophys. Rev.* **2010**, *2*, 55.
(8) Chu, P. K.; Chen, J. Y.; Wang, L. P.; Huang, N. *Mater. Sci. Eng., R* **2002**, *36*, 143.

(9) Siow, K. S.; Britcher, L.; Kumar, S.; Griesser, H. J. *Plasma Process. Polym.* **2006**, *3*, 392.
(10) Cretich, M.; Pirri, G.; Damin, F.; Solinas, I.; Chiari, M. *Anal. Biochem.* **2004**, *332*, 67.
(11) Chiari, M.; Cretich, M.; Corti, A.; Damin, F.; Pirri, G.; Longhi, R. *Proteomics* **2005**, *5*, 3600.
(12) Tuttle, P. V.; Rundell, A. E.; Webster, T. J. *Int J Nanomedicine* **2006**, *1*, 497.
(13) Lamb, S. B.; Stuckey, D. C. *Enzyme Microb. Technol.* **1999**, *24*, 541.
(14) Wentworth, D. S.; Skonberg, D.; Donahue, D. W.; Ghanem, A. *J. Appl. Polym. Sci.* **2004**, *91*, 1294.
(15) Kulagina, N. V.; Shaffer, K. M.; Ligler, F. S.; Taitt, C. R. *Sens. Actuators B* **2007**, *121*, 150.
(16) Ngundi, M. M.; Taitt, C. R.; Ligler, F. S. *Sens. Lett.* **2007**, *5*, 621.
(17) Inamori, K.; Kyo, M.; Matsukawa, K.; Inoue, Y.; Sonoda, T.; Tatematsu, K.; Tanizawa, K.; Mori, T.; Katayama, Y. *Anal. Chem.* **2008**, *80*, 643.
(18) Disney, M. D.; Seeberger, P. H. *Chem. Biol.* **2004**, *11*, 1701.
(19) Lock, E. H.; Walton, S. G.; Fernsler, R. F. *Plasma Process. Polym.* **2009**, *6*, 234.
(20) Darain, F.; Yager, P.; Gan, K. L.; Tjin, S. C. *Biosens. Biolelectronics* **2009**, *24*, 1744.
(21) Lock, E. H.; Petrovykh, D. Y.; Mack, P.; Carney, T.; White, R. G.; Walton, S. G.; Fernsler, R. F. *Langmuir* **2010**.
(22) Leonhardt, D.; Muratore, C.; Walton, S. G. *IEEE Trans. Plasma Sci.* **2005**, *33*, 783.
(23) Kulagina, N. V.; Shaffer, K. M.; Anderson, G. P.; Ligler, F. S.; Taitt, C. R. *Anal. Chim. Acta* **2006**, *575*, 9.
(24) Taitt, C. R.; North, S. H.; Kulagina, N. V., in *Peptide Microarrays: Methods and Protocols*; Cretich, M. Chiari, M., Eds.; Springer: New York, 2009; p 233.
(25) Alexander, M. R.; Jones, F. R. *Carbon* **1995**, *33*, 569.
(26) Petrat, F. M.; Wolany, D.; Schwede, B. C.; Wiedmann, L.; Benninghoven, A. *Surf. Interface Anal.* **1994**, *21*, 274.
(27) Petrat, F. M.; Wolany, D.; Schwede, B. C.; Wiedmann, L.; Benninghoven, A. *Surf. Interface Anal.* **1994**, *21*, 402.
(28) Lichtman, D.; Craig, J. H.; Sailer, V.; Drinkwine, M. *Appl. Surf. Sci.* **1981**, *7*, 325.
(29) Oh, S. J.; Cho, S. J.; Kim, C. O.; Park, J. W. *Langmuir* **2002**, *18*, 1764.
(30) Rossier, J. S.; Gokulrangan, G.; Girault, H. H.; Svojanovsky, S.; Wilson, G. S. *Langmuir* **2000**, *16*, 8489.
(31) Salonen, E. M.; Vaheri, A. *J. Immunol. Methods* **1979**, *30*, 209.
(32) Nygren, H.; Werthen, M.; Stenberg, M. *J. Immunol. Methods* **1987**, *101*, 63.
(33) Brewer, C. F.; Riehm, J. P. *Anal. Biochem.* **1967**, *18*, 248.
(34) Kulagina, N. V.; Lassman, M. E.; Ligler, F. S.; Taitt, C. R. *Anal. Chem.* **2005**, *77*, 6504.
(35) Shriver-Lake, L. C.; Charles, P. T.; Taitt, C. R. In *Biosensors and Biodetection: Methods and Protocols: Electrochemical and Mechanical Detectors, Lateral Flow and Ligands for Biosensors*; Rassoly, A., Herold, K. E., Eds.; Springer: New York, 2008; p 419.
(36) North, S. H.; Lock, E. H.; King, T. R.; Franek, J. B.; Walton, S. G.; Taitt, C. R. *Anal. Chem.* **2009**, *82*, 406.

AM100566E